Flow Visualization of Injection Process of R134a Scroll Compressor

I. Hwang[1]*, S. Lee[2], G. Lombardo[3,4], S. Rossi[3], D. Menegazzo[3,4], L. Fedele[3], S. Bobbo[3], M. S. Kim[1]

[1]Department of Mechanical Engineering, Seoul National University, Seoul (Republic of Korea)

[2]Institute of Advanced Machinery and Design, Seoul National University, Seoul (Republic of Korea)

[3]Construction Technologies Institute, National Research Council (CNR), Padova (Italy)

[4]Department of Industrial Engineering, University of Padua (UNIPD), Padova (Italy)

*Corresponding Author: hic0914@snu.ac.kr

ABSTRACT

This research delves into the intricate dynamics of the injection process within a visualization chamber designed to mimic a scroll compressor. Experimental investigations were conducted under diverse injection pressures, employing advanced image processing techniques to ensure a comprehensive analysis. The utilization of high-speed imaging allowed for the effective capture and visualization of the intricate details associated with the injection process. The application of the schlieren method played a pivotal role in accurately differentiating between R134a and CO2 based on variations in gas density. A meticulous methodology was employed to precisely track changes of the injection dynamics but also emphasized the considerable influence of both injection pressure and chamber pressure on the velocity of the injection tip. Furthermore, an examination of the cone angle under varying pressure conditions revealed notable observations. Specifically, as pressure differentials decreased, there was a discernible reduction in the injection stream. These findings contribute significantly to a deeper comprehension of vapor injection phenomena, providing valuable insights for the development of enhanced control and optimization strategies in refrigeration applications. The study paves the way for improved efficiency and performance in systems emulating scroll compressors.

1. INTRODUCTION

Climate change on a global scale has stimulated dialogues regarding climate-related initiatives. The objective of the 2015 Paris Agreement (COP21) was to restrict the increase in the mean global temperature to 1.5℃ via the mitigation of greenhouse gas emissions. Particularly in regard to heating, ventilation, and air conditioning (HVAC) systems, which account for 39% of a structure's energy consumption according to energy government of Australia (2012), carbon neutrality requires energy efficiency.

Heat pump systems are notable HVAC components that contribute significantly to the attainment of carbon neutrality, owing to their superior efficiency in comparison to conventional heating devices such as boilers. Heat pumps are attracting a growing amount of attention in Europe, prompting attempts to classify them as renewable energy technologies. Winter presents obstacles for heat pumps, as low temperatures increase the irreversibility of the compression process and diminish the bulk flow of refrigerant, resulting in a decrease in heating capacity and efficiency.

Utilizing intermediate refrigerant injection technology, which involves capacity variable compressors injecting additional refrigerant during compression, is one method for ensuring heating capacity at low temperatures. By reducing the temperature of compressor discharge and increasing the circulation of refrigerant, this technology improves the efficacy of heat pumps.

Ongoing research focuses on a variety of refrigerant injection technologies. An investigation was carried out by Aikins et al. (2013) utilizing two-stage compression technology, whereas Roh et al. (2012) examined the discharge characteristics of R407C refrigerant injection. A study was conducted by Heo et al. (2010) to examine the effects of flash tank-based refrigerant injection on the heating performance of heat pumps in frigid regions. Additionally, Xu et al. (2011) demonstrated the experimental application of injected refrigerant superheat as a control signal for the upper

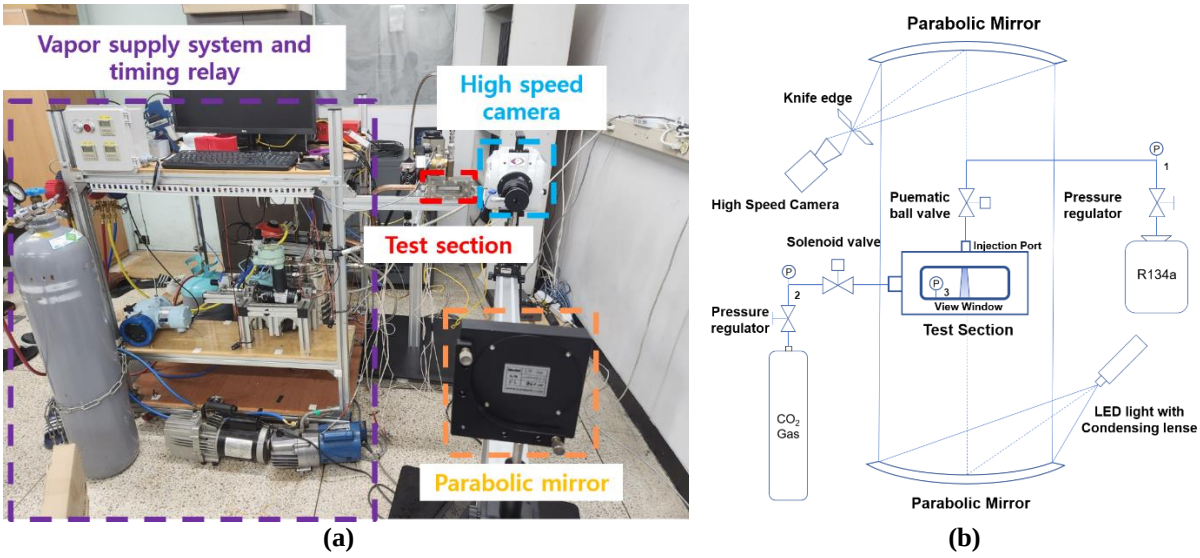

Figure 1: Schlieren experiment (a) apparatus and (b) schematic diagram

expansion valve. Furthermore, a time-dependent model was developed by Qiao et al. (2015) to analyze refrigerant injection heat pump systems that incorporate flash containers.

The primary objective of this research is to analyze the flow characteristics of the refrigerant injection process by determining the discharge angle and velocity of the refrigerant injection into the compressor.

2. EXPERIMENTAL INVESTIGATIONS SETUP

When refrigerant is introduced into a vapor injection scroll compressor via injection, compression occurs within the compressor concurrently with the injection operation. Injection occurs as a result of the transverse flow of refrigerant during compression and the resulting increase in internal pressure. In order to replicate this procedure, a pressurization-capable test chamber was built.

The experimental configuration illustrated in Figure 1 utilizes a Schlieren system comprising two mirrors to replicate the gas injection procedure within the compressor. The Schlieren method enables the visualization of gases through the utilization of light refraction induced by density differences as light traverses a gas. In order to improve the visibility of the injection procedure, R134a refrigerant gas was injected during the test segment, whereas CO2 gas was utilized to increase the pressure and generate density differences between the two gases.

The experimental procedure is as follows: condensed LED light is directed through a condensing lens onto the test section, functioning as a point source of illumination. Following reflection by parabolic mirrors, the light traverses the test section. Light refracts in the presence of a high gas density region within the test section, causing dark regions to appear in the image captured by a high-speed camera lens. This technique enables the distinction between regions containing R134a gas and those containing air or CO2 gas.

The test section has two ports and measures 25H × 25W × 116L. One of these ports is utilized to inject R134a refrigerant, while the other is compressed to generate pressure waves using CO2 in order to increase the test section's internal pressure. By means of transparent glass panels measuring 25H × 96L, light is permitted to traverse the test section.

In order to facilitate injection while CO2 is pressurized, a timing control device was developed to regulate the commencement of refrigerant injection and the timing of CO2 injection. A solenoid valve opens in response to a signal

Table 1: Page margins for manuscripts

Sensor	Type	Range	Uncertainty
P1, P2	Pressure Sensor	0 … 16 bar	±0.08 bar
P3	Pressure Sensor	0 … 5 bar	± 0.025 bar

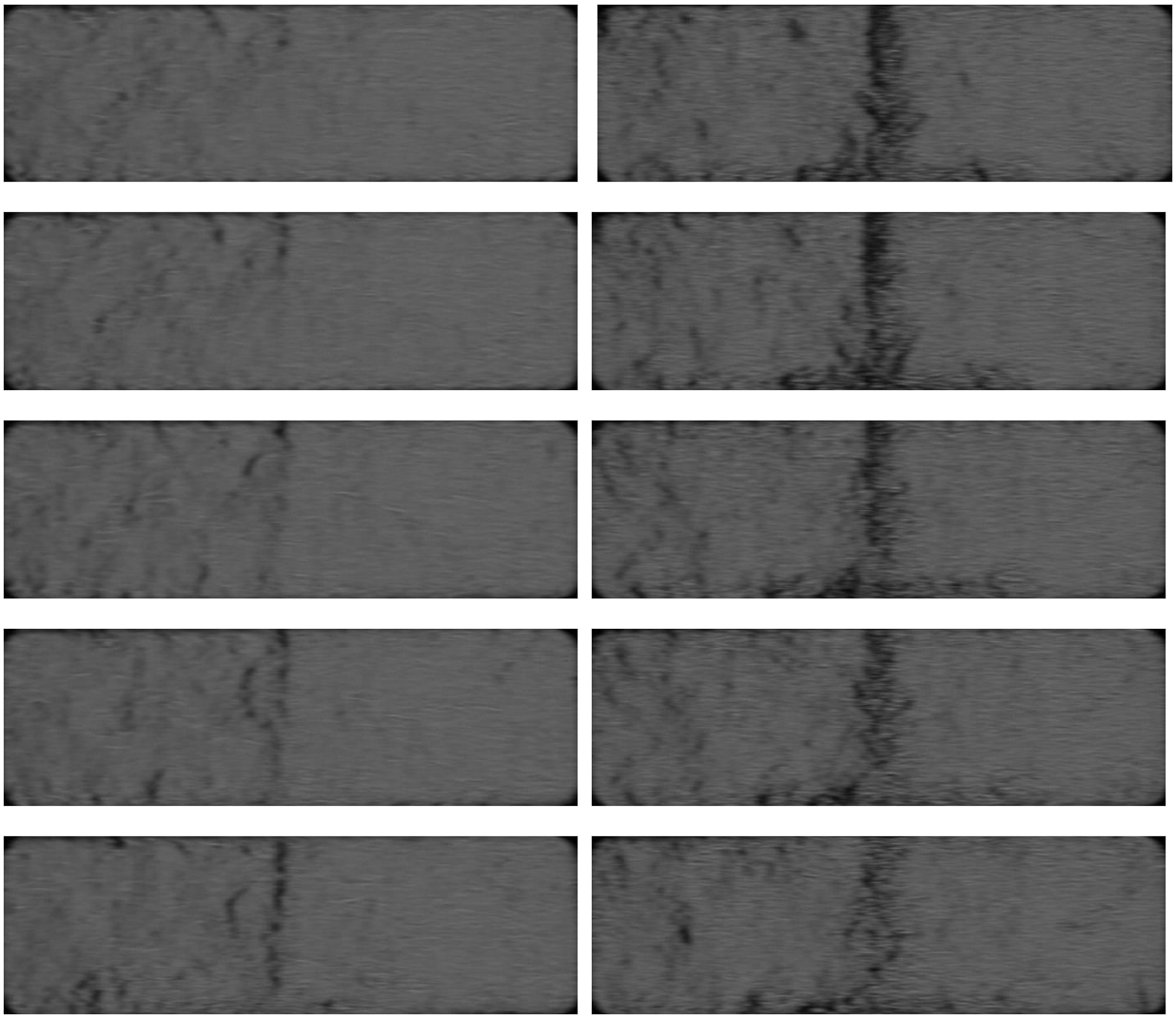

(a) (b)

Figure 2: Schlieren image of (a) initial injection process and (b) continuously decaying injection flow due to continuously increasing pressure in the chamber

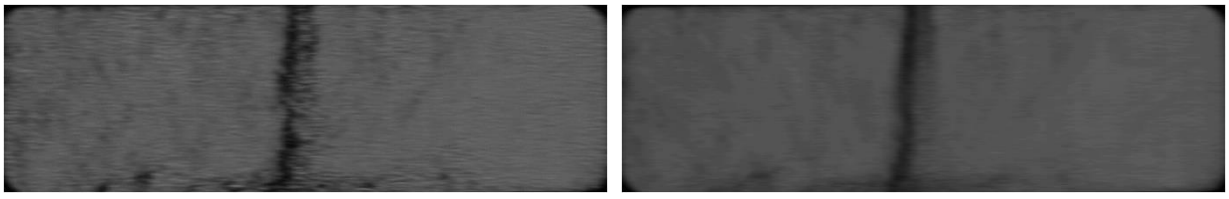

(a) (b)

Figure 3: Schlieren image of (a) before image processing (b) after image processing

from the timing relay in order to inject CO2, thereby increasing the test section's internal pressure. After a 50 milliseconds delay, R134a injection commences and continues for an additional 100 milliseconds. After that, CO2 is injected for an additional 50 milliseconds in order to simulate the compression process prior to and following injection. The injection procedure was documented using a Phantom v2640 camera, which has a maximum capturing rate of 6600 frames per second and a resolution of 2048 by 1920 pixels. The frame rate of the camera utilized in this investigation was 6000 FPS.

Pressure gauges were utilized to quantify the internal, injection port, and pressurizing CO2 pressures within the test section. A summary of the pressure gauges' uncertainty is provided in Table 1. In order to analyze the injection process under different pressure conditions, the injection pressures were adjusted at 0.5 bar increments from 2 bar to 4 bar, while the pressurizing CO2 was maintained at 2 bar, 3 bar, and 4 bar.

3. Results and Discussion

The photographs obtained using the high-speed camera depict the intensity, or luminosity, of each individual pixel. The initiation and completion of an injection are illustrated in Figure 2, wherein the injection pressure is 2 bar and the pressurizing gas pressure is 4 bar. The injection was scheduled to occur over a period of 600 frames, as the high-speed camera captured images at a rate of 6000 frames per second (FPS) and the duration of the injection was set to 100 milliseconds. The initial pressure in the test section is reduced relative to that of the injection site, thereby facilitating a seamless injection. However, intermittent injection occurs even when the injection port is open, as the internal pressure of the test section swiftly increases when the pressurizing gas pressure is high. This causes the pressure within the test section to exceed that of the injection port.

In order to comprehend the attributes of the injection procedure, a steady analysis of the injected refrigerant flow is required. The flow is affected when conducting experiments in a test section that simulates a scroll compressor due to the reflection of refrigerant on the lower portion of the test section. As a consequence, the administered gas flow becomes unreliable, thereby impeding the ability to precisely discern the trend from a single frame. As a result, the analysis was performed by calculating the mean intensity of the five frames preceding and following the reference frame. The reference frame is juxtaposed with the averaged frame in Figure 3. In comparison to the unprocessed data, the processed image reveals that the pressurizing CO2 has a lower intensity, and the injection zone's boundaries appear more stable.

3.1 Injection Velocity

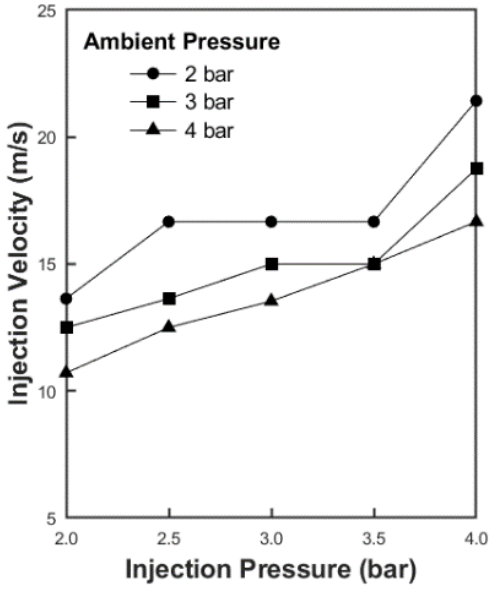

Figure 4: Injection velocity under various pressure conditions

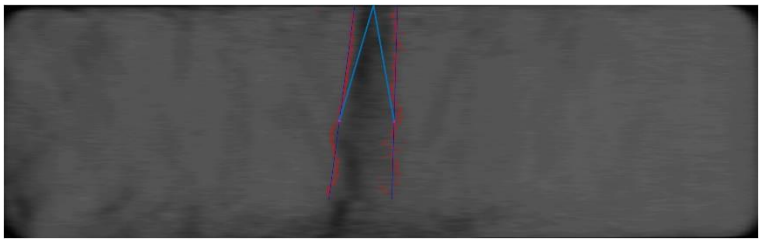

Figure 5: Injection boundary (red dot) and 1-D fitting diagram (blue line)

In order to quantify the velocity of refrigerant injection, it is necessary to have data regarding the height of the test section and the duration required for the injection tip to descend to the bottom of the test section subsequent to the initiation of injection. The time constant utilized in this investigation is 1/6000 second per frame, while Equation (1) can be employed to compute the tip velocity.

$$v_{inj} = h_{test}/(n \times t_F) \tag{1}$$

The injection velocity was determined through the manipulation of both the injection pressure and the pressure of the pressurizing CO2. The obtained data are illustrated in Figure 4. An elevation in injection pressure generally results in an increase in injection velocity. This is because, due to the pressure difference within the test section, the higher pressure of the injected refrigerant causes a quicker injection velocity. The internal pressure of the test section increases at a faster rate as the pressure of the pressurizing gas rises; this results in a decrease in the pressure differential between the injection port and the test section. Hence, there exists an inverse relationship between injection velocity and ambient pressure.

3.2 Injection Angle

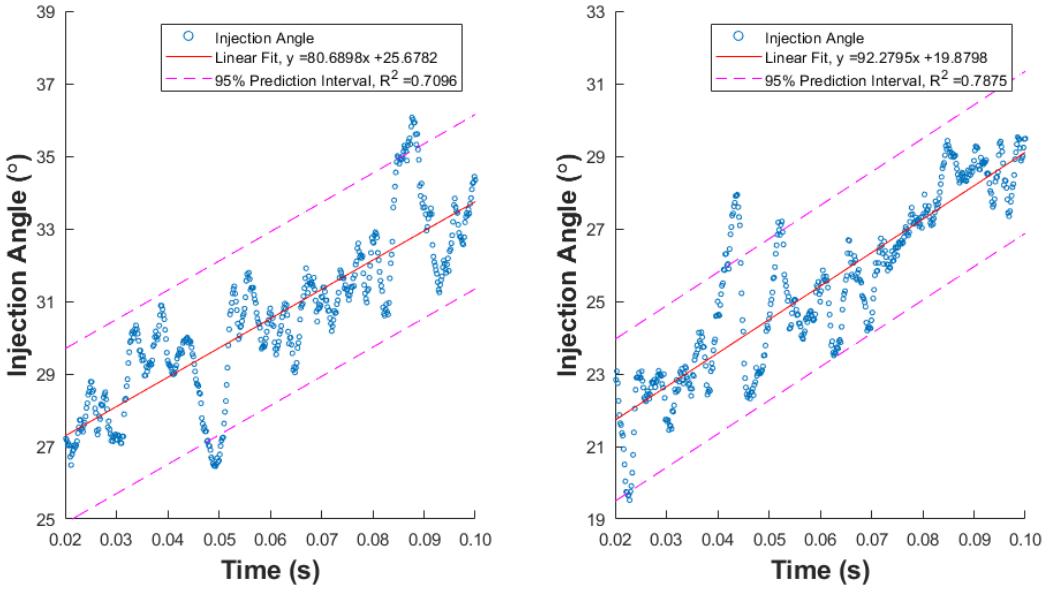

(a) (b)

Figure 6: Time dependent injection angle at (a) injection pressure 3 bar ambient pressure 3 bar (b) injection pressure 4 bar ambient pressure 4 bar

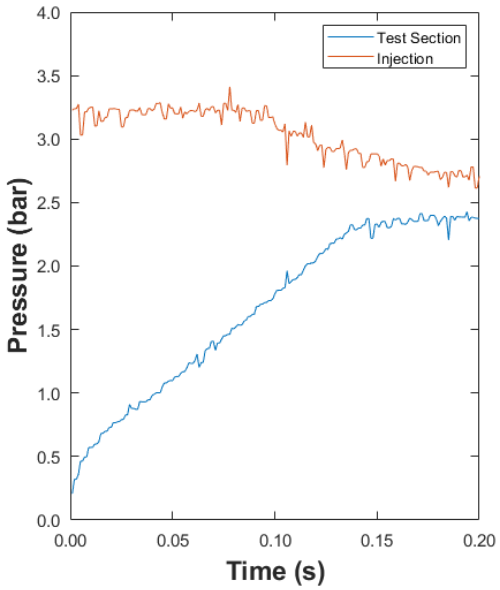

Figure 7: Time dependent injection pressure and pressure inside of the test section

Raju et al. (2015) determined the injection angle to be one-third of the STP, whereas Roh et al. (2012). determined it to be half the STP. While several approaches have been suggested in prior research to quantify the injection angle, their application presents a significant obstacle in the present investigation. In contrast to prior investigations that utilized chambers of adequate size and elevated pressure to conduct injections, the present study employs pressurization and utilizes a chamber of restricted dimensions. Furthermore, the movement of injected refrigerant becomes unsteady due to the influence of two factors: the reflection of refrigerant gas on the floor of the test section and the flow of CO2 introduced for pressurization. In order to mitigate this instability, frame averaging was implemented for the purpose of analysis. Nevertheless, relying on a single frame to analyze the real-time instability of the refrigerant flow may result in substantial inaccuracies. This study therefore introduces a novel technique for determining the injection angle.

The outcomes of the injection angle measurement procedure, which comprises three stages, are illustrated in Figure 5. Prior to proceeding, the injection stream boundary must be determined. The differentiation between CO2 and R134a is enhanced via image processing. The boundary of R134a presence is determined by identifying the area within the injection zone where the intensity abruptly changes, given that R134a appears relatively darkened. In Figure 5, the boundaries of the injection zone are denoted by red dots.

The observed boundary is subsequently approximated using a one-dimensional line. Using reference points at the measurement height to determine the injection angle may result in considerably divergent conclusions as a consequence of flow instability. Consequently, the directionality of the injected stream can be better comprehended by fitting the injection boundary into a one-dimensional equation; consequently, determining the injection angle using this fitting line provides a more precise method.

In conclusion, the injection angle is defined as the intersection of the initial coordinate of the injection and the midpoint of the fitted line. The reference point was established at the midpoint of the injection height, employing the procedure described by Roh et al. (2012).

The injection angle was determined at different pressure levels utilizing this technique; the outcomes are illustrated in Figure 6. The temporal evolution of the injection angle is illustrated in Figure 6. In this figure, the angle changes from 4 bar at the injection pressure to 3 bar at the ambient pressure. An increase in the injection angle is evident as time progresses. This phenomenon is distinct from those that occur when injection is performed at elevated pressure in adequately large chambers. The temporal evolution of the pressures at the injection port and within the test section is illustrated in Figure 7. Both the injection pressure and the ambient pressure are maintained at 3 bar. The data presented in the graph demonstrates that as time passes, the pressure within the test section increases while the pressure at the injection port decreases. This is the result of the gradual decrease in refrigerant gas volume within the pipeline, which causes an accompanying reduction in pressure. Additionally, the presence of CO2 and R134a gases within the test segment contribute to an elevation in pressure within the pipeline.

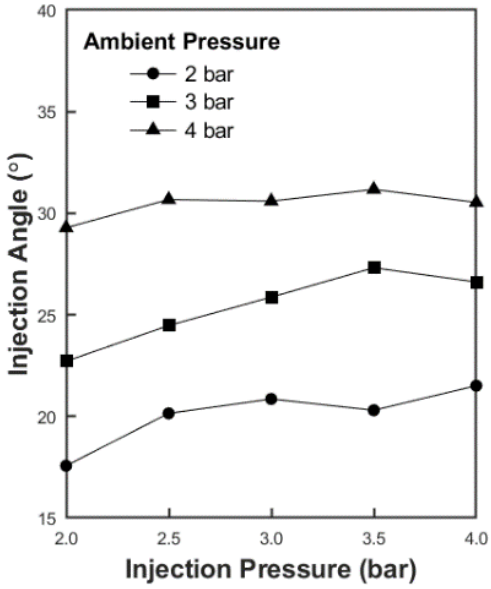

Figure 8: Injection angle at various pressures

Therefore, subsequent research indicates that as the ambient pressure increases and the injection pressure decreases, the injection angle ought to diminish. The experimental results, on the other hand, indicate that the injection angle increases progressively with time. This phenomenon is caused by variations in the injection angle caused by the refrigerant gas flow reflected from the test section and the pressurized gas flow. The average change in cone angle over time is depicted in Figure 8. The data suggests that an increase in both ambient pressure and injection pressure corresponds to a corresponding increase in angle. Alternatively stated, the injection angle increases as the flow velocity and intensity of the injection within the test section increase.

4. CONCLUSIONS

This paper presented an analysis of injection characteristics of scroll compressor under various conditions. The characteristics of the flow within the injection scroll compressor differ from those of straightforward injection processes, as a result of the fluid flow during pressurization and the downward propagation of flow. Therefore, it is imperative to distinguish and create models that simulate the scroll compressor with precision. Subsequent investigations strive to construct a Computational Fluid Dynamics (CFD) model that more precisely characterizes the scroll compressor and simulates the injection procedure.

NOMENCLATURE

v	velocity	(m/s)
h	height	(m)
n	number of frames	(–)
t_F	time per one frame	(s)

Subscript

inj	injection
test	test section

REFERENCES

Aikins, K. A., Lee, S. H., and Choi, J. M. (2013). Technology review of two-stage vapor compression heat pump system. *International Journal of Air-Conditioning and Refrigeration*, 21(03), 1330002

Roh, C. W., Kim, M. S. (2012). Macroscopic spray behavior and atomization characteristics of R407c injection. *International Journal of Air-Conditioning and Refrigeration*, 20(03), 1250009.
Heo, J., Jeong, M. W., Kim, Y. (2010). Effects of flash tank vapor injection on the heating performance of an inverter-driven heat pump for cold regions. *International Journal of Air-Conditioning and Refrigeration*, 33(4), 848-855.
Xu, X., Hwang, Y., Radermacher, R. (2011). Transient and steady-state experimental investigation of flash tank vapor injection heat pump cycle control strategy. *International journal of refrigeration*, 34(8), 1922-1933.
Qiao, H., Aute, V., Radermacher, R. (2015). Transient modeling of a flash tank vapor injection heat pump system–Part I: Model development. *International journal of refrigeration*, 49, 169-182.
Raju, V. R. K., Rao, S. S. (2015). Effect of fuel injection pressure and spray cone angle in DI diesel engine using CONVERGETM CFD code. *Procedia Engineering*, 127, 295-300.